学位論文

Regulation of membrane KCNQ1/KCNE1 channel density by sphingomyelin synthase 1

（スフィンゴミエリン合成酵素１による KCNQ1/KCNE1 チャネルの調節作用）

ウ　メイクイ
Wu　Meikui

熊本大学大学院医学教育部博士課程医学専攻
HIGO プログラム４年コース

指導教員
宋　文杰 教授

熊本大学大学院医学教育部博士課程医学専攻知覚生理学

２０１７年９月

学　位　論　文

論文題名　：　Regulation of membrane KCNQ1/KCNE1 channel density by sphingomyelin synthase 1
（スフィンゴミエリン合成酵素１による KCNQ1/KCNE1 チャネルの調節作用）

著 者 名　：　ウ　メイクイ
Wu　Meikui

指導教員名　：　熊本大学大学院医学教育部博士課程医学専攻知覚生理学　宋　文杰　教授

審査委員名　：　分子生理学担当教授　富澤　一仁
分子脳科学担当教授　岩本　和也
形態構築学担当教授　福田　孝一
神経分化学担当准教授　太田　訓正

２０１７年９月

Regulation of Membrane KCNQ1/KCNE1 Channel Density by Sphingomyelin Synthase 1

Meikui Wu[1, 2], Makoto Takemoto[1], Makoto Taniguchi[3], Toru Takumi[4], Toshiro Okazaki[3,5], Wen-Jie Song*[1, 2]

[1] Department of Sensory and Cognitive Physiology, Graduate School of Medical Sciences, Kumamoto University, Kumamoto, Japan

[2] Program for Leading Graduate Schools HIGO Program, Kumamoto University, Kumamoto, Japan

[3] Medical Research Institute, Kanazawa Medical University, Ishikawa, Japan

[4] RIKEN Brain Science Institute, Wako, Japan

[5] Department of Hematology and Immunology, Kanazawa Medical University, Ishikawa, Japan

Keywords: KCNQ1, KCNE1, Sphingomyelin synthase, PKD

Running head: SMS1 regulation of KCNQ1/KCNE1

Figures: 7; Tables: 0

* Correspondence to:

Wen-Jie Song, Department of Sensory and Cognitive Physiology, Graduate School of Medical Sciences, Kumamoto University, Kumamoto 860-8556, Japan.

Tel: +81-96-373-5056; Fax: +81-96-373-5060; E-mail: song@kumamoto-u.ac.jp

ABSTRACT

Sphingomyelin synthase (SMS) catalyzes the conversion of phosphatidylcholine and ceramide to sphingomyelin and diacylglycerol. We previously showed that SMS1 deficiency leads to a reduction in expression of the K^+ channel KCNQ1 in the inner ear, causing hearing loss. However, it remains unknown whether this change in expression is attributable to a cellular process or a systemic effect in the knockout animal. Here, we examined whether manipulation of SMS1 activity affects KCNQ1/KCNE1 currents in individual cells. To this end, we expressed the KCNQ1/KCNE1 channel in human embryonic kidney 293T cells, and evaluated the effect of SMS1 manipulations on the channel using whole-cell recording. Application of tricyclodecan-9-yl-xanthogenate, a non-specific inhibitor of SMSs, significantly reduced current density and altered channel voltage dependence. Knockdown of SMS1 by an shRNA, however, reduced current density alone. Consistent with this, overexpression of SMS1 increased the current density without changing channel properties. Furthermore, application of protein kinase D (PKD) inhibitors also suppressed current density without changing channel properties; this effect was non-additive with that of SMS1 shRNA. These results suggest that SMS1 positively regulates KCNQ1/KCNE1 channel density in a PKD-dependent manner.

INTRODUCTION

The slowly activating, delayed rectifier potassium channel encoded by KCNQ1 (α subunit, also known as Kv7.1) and KCNE1 (β subunit, also known as Isk or minK) plays important roles in a number of organs including the inner ear, heart, pancreas, and brain (reviewed in Refs. 1, 15, 19). In the heart, the KCNQ1/KCNE1 channel (also known as the cardiac I_{Ks} channel) is necessary for the termination of action potentials (5, 30, 42), and loss of function of the I_{Ks} channel causes prolongation of the QT interval in the ECG (26). In the inner ear, KCNQ1/KCNE1 channels are expressed exclusively on the apical surface of marginal cells of the stria vascularis (14, 29), maintaining the endocochlear potential and thereby the high sensitivity of the inner ear to sound. Dysfunction of KCNQ1/KCNE1 channels in the inner ear causes hearing impairment or congenital deafness (3, 15, 27). Understanding how KCNQ1/KCNE1 channels are regulated is therefore of profound biological significance.

We previously showed that KCNQ1 expression in the inner ear may be subject to regulation by sphingomyelin synthase 1 (SMS1) (21). SMS1 is one of the two isoforms of the enzyme that catalyzes the conversion of phosphatidylcholine and ceramide to sphingomyelin and diacylglycerol (DAG) (reviewed in Refs. 18, 38). We showed that SMS1 deficiency results in hearing impairment, which is attributable to a reduction in endocochlear potential caused by aberrant KCNQ1 protein expression in the marginal cells of the stria vascularis of the inner ear (21). Although these observations raise the possibility that SMS1 has a regulatory role in

KCNQ1 expression, it is not known whether SMS1 affects KCNQ1 via a cellular mechanism, i.e., within the marginal cells, or indirectly via systemic pathways. Here, we examined whether manipulation of SMS1 activity affects KCNQ1/KCNE1 current at the cellular level. To this end, we expressed KCNQ1/KCNE1 channels in human embryonic kidney 293T (HEK293T) cells, which express little endogenous potassium current, and evaluated the effect of SMS1 manipulations on the channel using whole-cell recordings. Our results show that SMS1 positively regulates KCNQ1/KCNE1 channel density at the cellular level, without changing channel properties. Regulation of SMS1 activity therefore has therapeutic potential in hearing, cardiac, and metabolic disorders.

MATERIALS AND METHODS

Plasmids

We constructed a plasmid for SMS1 overexpression by inserting human SMS1 cDNA, tagged with Myc at the C terminal, into the pLPCX plasmid vector (Takara, Shiga, Japan) at the EcoRI/NotI site. Plasmids for short-hairpin RNA (shRNA) against SMS1, and control (scrambled) shRNA, were constructed previously (16). We constructed a FLAG-tagged human KCNE1 plasmid by inserting cDNA encoding human KCNE1, tagged with FLAG at the C terminal, into the pcDNA3 plasmid vector (Thermo Fisher Scientific, Waltham, MA, USA) (24, 40). A GFP-tagged human KCNQ1 cDNA plasmid (RG219869) was purchased from

OriGene (Rockville, MD, USA). All plasmid solutions for transfection were prepared using the PureLink™ HiPure Plasmid Maxiprep Kit (Thermo Fisher Scientific).

Cell culture and plasmid transfection

HEK293T cells were maintained in DMEM with 10% FBS, in 35-mm dishes. One day after plating the cells (1×10^5 cells per dish), KCNQ1 and KCNE1 plasmids (3 μg of each) were diluted in Opti-MEM® I Reduced Serum Medium (Thermo Fisher Scientific) and transfected by mixing with either 5 μL Lipofectamine 3000 transfection reagent (Thermo Fisher Scientific; for CID-2011756 and phorbol 12-myristate 13-acetate (PMA) experiments) or 8 μL Lipofectamine 2000 transfection reagent (Thermo Fisher Scientific; for all other experiments). We added 2.2 μg of SMS1 plasmid for overexpression experiments, and 3 μg SMS1 shRNA plasmid for knockdown experiments. The empty vector (pLPCX) and scrambled shRNA plasmids were used as controls. Whole cell recordings were performed 48 h post-transfection. Approximately 5 h before recording, cells were transferred to poly-L-lysine-coated coverslips in DMEM containing 10% FBS.

Reverse Transcription-Polymerase Chain Reaction

To examine whether SMS1 knockdown/overexpression had altered SMS1 mRNA level, we measured the SMS1/beta-actin mRNA ratio by reverse transcription-polymerase chain reaction (RT-PCR) analysis. We also measured the SMS2/beta-actin mRNA ratio to test the specificity of our shRNA. Total RNA was

111 isolated from HEK293T cells using the RNeasy Plus Mini kit (Qiagen, Hilden,
112 Germany). Concentrations were normalized to the respective control groups. RT was
113 carried out using the SuperScript® III First-Strand Synthesis System for RT-PCR kit
114 (Thermo Fisher Scientific), with oligo-dT as the primer. All procedures followed the
115 manufacturers' instructions.

116 PCR was carried out using KOD-FX DNA polymerase (Toyobo, Osaka,
117 Japan), with the following primers: human beta-actin (forward), 5′-GCA CAG AGC
118 CTC GCC TTT GCC GAT-3′; (reverse): 5′-CTC CTT AAT GTC ACG CAC GAT
119 TTC-3′; human SMS1 (forward): 5′-TGG CAG ACT GGC TGC TGG AGA AT-3′;
120 (reverse): 5′-GTC ATT CAC CAG CCG GCT GTA TT-3′; human SMS2 (forward): 5′-
121 CCA GTG ATC CTA CGA ACA CTT AT-3′; (reverse): 5′-CAT TGT CTT CAA TCT
122 TCT GA-3′. PCR products were stained with ethidium bromide after agarose gel
123 electrophoresis. Images were obtained with an ultraviolet transilluminator
124 (CSF-20BF-S; Cosmo Bio, Tokyo, Japan) and a digital camera (DC120, Kodak);
125 fluorescence intensity was measured using ImageJ 1.45 (National Institutes of Health,
126 Bethesda, MD, USA).

127

128 *Electrophysiology*

129 Whole-cell recordings of K^+ currents were performed according to our
130 previously published methods (12, 36). GFP-labeled (transfected) cells were
131 randomly selected for recording. The recording chamber was perfused with a
132 background solution containing (in mM) 140 NaCl, 2 KCl, 1 $CaCl_2$, 2 $MgCl_2$, 10

Glucose, 15 HEPES; pH adjusted to 7.4 with NaOH; osmolarity was 295–300 mOsm/l. The external solution consisted of (in mM) 140 NaCl, 2 KCl, 2 $MgCl_2$, 10 Glucose, 10 HEPES; pH = 7.4 with NaOH; 295–300 mOsm/l. Ca^{2+} was excluded from the external solution to eliminate Ca^{2+} currents. During recording, cells were bathed in extracellular solution applied via a gravity-fed capillary perfusion array positioned about 2 mm away from the cell under study. The internal solution consisted of (in mM) 120 potassium gluconate, 3 $MgCl_2$, 10 HEPES, 10 EGTA, 2 ATP, 12 phosphocreatine, 0.2 GTP; pH = 7.2–7.3 with KOH; 275–285 mOsm/l. Room temperature was controlled at 25–27 °C during recording.

Recordings were obtained with an Axon Instruments patch clamp amplifier (Axopatch 200B, Molecular Devices, Foster City, CA, USA) and were controlled and monitored with a computer running pCLAMP 7.0 with a 125 kHz interface (Molecular Devices). Electrode resistances were typically 3–6 MΩ in the bath. The tip potentials of the patch pipets were zeroed prior to seal formation. After seal rupture, the series resistance (7–15 MΩ) was compensated (> 80%) and periodically monitored. The liquid junction potential between the pipet solution and the bath solution was not compensated. KCNQ1 and KCNQ1/KCNE1 currents were evoked by depolarization voltage steps. Unstable recordings were excluded from analysis.

Drugs

To inhibit SMS activity, we added tricyclodecan-9-yl-xanthogenate (D609, Sigma, St. Louis, MO, USA; 300 μM), to the culture dishes for 6 h (4, 37). Control

cells received DMSO vehicle (0.05%) for the same period of time. To inhibit protein kinase D (PKD), we added either CID-755673 or CID-2011756 (Tocris, Bristol, UK; 40 μM) to the cultures for 6 h (9, 33, 34, 48), and control cells received DMSO (0.05%). The effect of PMA (Sigma-Aldrich; 50 nM) was also tested by adding the drug to the cultures for 6 h, and control cells received DMSO vehicle (0.05%).

Data analysis

Recordings were analyzed using AxoGraph (AxoGraph, Berkeley, CA, USA) and Matlab (Mathworks, Natick, MA, USA). KaleidaGraph (Synergy Software, Reading, PA, USA) was used for drawing box plots and for Boltzmann fitting. Conductance–voltage relationships were derived from tail currents. Sample statistics are given as the mean ± SEM, unless stated otherwise. The Wilcoxon signed-rank test was used to compare samples.

RESULTS

Expression of KCNQ1/KCNE1 currents in HEK293T cells

We used HEK293T cells as models because they express low levels of depolarization-activated K^+ currents (15) (Fig. 1A). The peak current density was 7.6 ± 0.8 pA/pF at 50 mV (n = 10). Endogenous K^+ currents in HEK293T cells activated with a short time constant of 25.7 ± 3.2 ms at 10 mV (n = 10). When KCNQ1 was expressed alone, peak current density showed no significant increase (8.6 ± 0.9

177 pA/pF at 50 mV; $p > 0.05$, n = 13; Fig. 1B), and channel activation, at 10 mV, could also
178 be described by a single exponent, though with longer time constants than in control
179 cells (37.4 ± 3.5 ms; $p < 0.05$, n = 13). In agreement with previous reports (32),
180 co-expression of KCNQ1 and KCNE1 in HEK293T cells resulted in much slower
181 currents (Fig. 1C), which had a typical sigmoidal shape in response to depolarization
182 voltage steps (15, 25); also in agreement with these previous studies, the channel
183 deactivated slowly after termination of the depolarization pulse (Fig. 1C, arrow). The
184 peak current density (47.9 ± 11.1 pA/pF at 50 mV; n = 25) was significantly greater
185 than that of control cells ($p < 0.01$; Fig. 1D). Therefore, with KCNQ1/KCNE1
186 expression, 84% ((47.9–7.6)/47.9) of depolarization-activated K^+ current in HEK293T
187 cells was KCNQ1/KCNE1 current, similar to that reported previously (15). We
188 subsequently used this model system to study the mechanisms of KCNQ1/KCNE1
189 current regulation by SMS1.
190
191 *Effects of D609 treatment on KCNQ1/KCNE1 currents*
192 To determine whether SMS1 affects KCNQ1/KCNE1 currents, we first
193 explored the effects of D609, a nonspecific inhibitor of SMS1 (reviewed in Ref. 2).
194 Cells treated with D609 for 6 h had much lower current density (Fig. 2B) than control
195 cells (Fig. 2A). At 110 mV, peak current density was 58.7 ± 8.1 pA/pF (n = 9) in the
196 D609-treated cells, significantly lower than that in the control group (255.6 ± 43.8
197 pA/pF; $p < 0.001$, n = 10; Fig. 2C).
198 To examine how D609 alters channel voltage dependence, the

conductance–voltage relationships in cells of both groups were fitted, for descriptive purposes, with a single Boltzmann function: $g = g_{max}/(1+\exp(-(V-V_h)/V_c))$, where g_{max} is the maximum conductance density, V_h is the half-activation voltage, and V_c is the slope factor (35) (Fig. 2D). D609 markedly shifted the half-activation voltage to negative potential (control, 92.1 ± 4.4 mV, n = 10; D609, 12.3 ± 9.7 mV, n = 9; $p < 0.01$; Fig. 2E, F) and reduced the maximum conductance density (control, 24.4 ± 4.0 pS/μm², n = 10; D609, 1.9 ± 0.3 pS/μm², n = 9; $p < 0.01$; Fig. 2F). No significant change was found for the slope factor (control, 26.5 ± 1.2 mV, n = 10; D609, 24.6 ± 2.7 mV, n = 9; $p > 0.05$; Fig. 2F).

These results suggest the possibility that SMS1 regulates the expression and voltage dependence of KCNQ1/KCNE1 channels.

Regulation of KCNQ1/KCNE1 currents by SMS1

To manipulate SMS1 activity more specifically, we used an shRNA to knock down SMS1 expression. Transfection of the SMS1 shRNA plasmid resulted in significantly less SMS1 mRNA than in the scrambled control ($p < 0.05$, n = 7; Fig. 3A). The degree of mRNA reduction was similar to that reported by a real-time PCR study that used the same shRNA (16). The knockdown effect was specific to SMS1 because no change was observed in the amount of SMS2 mRNA in the same experiment ($p > 0.05$, n = 7; Fig. 3A).

KCNQ1/KCNE1 current density was significantly lower after transfection of the SMS1 shRNA plasmid than after scrambled control plasmid transfection (at 110

mV: SMS1 shRNA, 155.2 ± 21.5 pA/pF, n = 24; control, 260.4 ± 26.5 pA/pF, n = 24; $p < 0.05$; Fig. 3B–D). However, the effect of SMS1 knockdown was limited to channel density. Conductance density–voltage relationships were fitted with the Boltzmann function to reveal significantly lower maximum conductance density in the SMS1 shRNA group than in the scrambled control group (control: 32.2 ± 3.5 pS/μm², n = 24; shRNA: 21.4 ± 4.0 pS/μm², n = 24; $p < 0.05$), but no change in half-activation voltage or slope factor was observed (V_h: shRNA, 108.0 ± 2.4 mV, n = 24; control, 104.3 ± 2.2 mV, n = 24; $p > 0.05$. V_c: shRNA, 23.0 ± 0.9 mV, n = 24; control, 23.3 ± 0.4 mV, n = 24; $p > 0.05$; Fig. 4A, B). Furthermore, time-dependent current change during activation at 110 mV and during deactivation at −40 mV in knockdown cells was in close agreement with that in control cells (Fig. 4C, D).

Conversely, overexpression of SMS1 resulted in a greater amount of SMS1 mRNA compared with the empty vector control ($p < 0.05$, n = 6; Fig. 5A, left side). This effect was specific to SMS1, because no change in SMS2 mRNA level was detected in the same experiment ($p > 0.05$, n = 6; Fig. 5A, right side).

Cells overexpressing SMS1 had significantly higher KCNQ1/KCNE1 current density than empty vector cells (at 110 mV: overexpression, 356.1 ± 95.2 pA/pF, n = 14; control, 211.9 ± 28.4 pA/pF, n = 18; $p < 0.05$; Fig. 5B–D). Similarly to the knockdown experiments, we found no change in channel voltage dependence (V_h: overexpression, 95.9 ± 4.3 mV, n = 14; control, 110.1 ± 15.5 mV, n = 18; $p > 0.05$. V_c: overexpression, 24.4 ± 0.8 mV, n = 14; control, 27.0 ± 2.5 mV, n = 18; $p > 0.05$), or in kinetics in the overexpression experiments (data not shown). The maximum

conductance density in cells overexpressing SMS1 was not statistically significantly different from that in empty vector cells (overexpression: 65.5 ± 19.7 pS/μm^2, n = 14; control: 27.7 ± 5.0 pS/μm^2, n = 18; p = 0.09), probably owing to the large variance of the overexpression group.

Together, the results of the knockdown and overexpression experiments suggest that SMS1 positively regulates KCNQ1/KCNE1 channel expression without affecting channel properties.

Suppression of KCNQ1/KCNE1 currents by PKD inhibitors

We next investigated the cellular mechanism by which SMS1 regulates the expression of KCNQ1/KCNE1 channels. SMS1 is known to reside in the Golgi apparatus and catalyzes the conversion of phosphatidylcholine and ceramide to sphingomyelin and DAG (18, 38). Because SMS1 changed KCNQ1/KCNE1 current density only, without changing channel properties, it is likely that SMS1 affects the trafficking of channel proteins to the cytoplasmic membrane, rather than modifying the channel proteins themselves. We therefore focused on the reaction product DAG, and speculated that DAG might lead to the regulation of KCNQ1/KCNE1 expression via the DAG-binding kinase, PKD (6). We found that the PKD inhibitor CID-755673 (9, 33) significantly reduced the current density of the KCNQ1/KCNE1 channel (Fig. 6A–C). Similarly to that observed after SMS1 downregulation, the effect of CID-755673 was limited to a reduction in channel density (at 110 mV: CID-755673, 144.2 ± 17.2 pA/pF, n = 12; control, 266.8 ± 43.6 pA/pF, n = 14; $p < 0.05$). Analysis of

265 the channel conductance–voltage relationship revealed that CID-755673 significantly
266 reduced the maximum conductance (control, 28.7 ± 5.0 pS/μm², n = 14; CID-755673,
267 15.9 ± 3.0 pS/μm², n = 12; $p < 0.05$) but had no effect on half-activation voltage or
268 slope factor (V_h: control, 92.6 ± 3.4 mV, n = 14; CID-755673, 94.4 ± 3.6 mV, n = 12; $p >$
269 0.05. V_c: control, 24.6 ± 0.7 mV, n = 14; CID-755673, 24.1 ± 0.9 mV, n = 12; $p > 0.05$; Fig.
270 6D, E).

271 To determine whether SMS1 and PKD regulate KCNQ1/KCNE1 channel
272 density via a common signaling pathway, we tested whether the effects of SMS1
273 knockdown and PKD inhibition were additive (Fig. 7). Knockdown by SMS1 shRNA
274 plus CID-755673 suppressed current density to a similar level as SMS1 shRNA
275 knockdown alone (at 110 mV: control, 266.8 ± 43.6 pA/pF, n = 14; shRNA, 147.3 ± 36.9
276 pA/pF, n = 12; shRNA+CID-755673, 133.8 ± 22.5 pA/pF, n = 12; $p < 0.05$ for control vs.
277 shRNA and for control vs. shRNA+CID-755673; $p > 0.05$ for shRNA and
278 shRNA+CID-755673). Similar changes were found for g_{max} derived from Boltzmann
279 fits (control, 28.7 ± 5.0 pS/μm², n = 14; shRNA, 14.1 ± 5.1 pS/μm², n = 12;
280 shRNA+CID-755673, 12.7 ± 2.2 pS/μm², n = 12; $p < 0.05$ for control vs. shRNA and for
281 control vs. shRNA+CID-755673; $p > 0.05$ for shRNA vs. shRNA+CID-755673).

282 To further test the involvement of PKD in the regulation of KCNQ1/KCNE1
283 channels by SMS1, we studied the effect of another antagonist of PKD, CID-2011756
284 (34, 48). Similarly to CID-755673, CID-2011756 significantly reduced current density
285 at 110 mV (CID-2011756, 140.7 ± 24.6 pA/pF, n = 33; control, 321.2 ± 22.8 pA/pF, n =
286 56; $p < 0.05$; data not shown). Furthermore, the suppressive effect of CID-2011756

was also found to be non-additive with the effect of SMS1 knockdown (at 110 mV: control, 340.1 ± 37.4 pA/pF, n = 41; shRNA, 253.1 ± 29.1 pA/pF, n = 56; shRNA+CID-2011756, 220.3 ± 32.0 pA/pF, n = 41; $p < 0.05$ for control vs. shRNA and for control vs. shRNA+CID-2011756; $p > 0.05$ for shRNA vs. shRNA+CID-2011756).

These results suggest that PKD works downstream of SMS1 in the regulation of KCNQ1/KCNE1 channels. An immediate question is whether DAG analogues mimic the effects of SMS1. To address this, we tested the effect of a phorbol ester, PMA (50 nM) (17, 43). However, no significant effect of PMA was found on current density (at 110 mV: control, 302.1 ± 49.3 pA/pF, n = 32; PMA, 258.0 ± 39.2 pA/pF, n = 34; $p > 0.05$; data not shown).

DISCUSSION

We have shown here that knockdown of SMS1 in HEK293T cells downregulates KCNQ1/KCNE1 channel density without changing channel voltage dependence. Consistent with this, overexpression of SMS1 increased current density only. Furthermore, we have demonstrated that inhibition of PKD reduces KCNQ1/KCNE1 channel density, and that this effect is not additive with that of SMS1 knockdown. Our results suggest that SMS1 positively regulates KCNQ1/KCNE1 channel density via a PKD-dependent pathway.

SMS1 positively regulates KCNQ1/KCNE1 current expression

All lines of evidence obtained here (D609 treatment, SMS1 knockdown, SMS1 overexpression) support the notion that SMS1 positively regulates the expression of KCNQ1/KCNE1 channels.

The alteration in channel voltage dependence by D609 was not observed after overexpression or knockdown of SMS1, and D609 suppressed the current more drastically than SMS1 knockdown (compare Fig. 2C to Fig. 3D). These may be attributable to the effect of D609 on other enzymes including SMS2 and phosphatidylcholine-specific phospholipase C (2); it is also possible that D609 acts directly on the channel. These possibilities need to be explored in future studies.

Because KCNQ1/KCNE1 channels in this study appeared not fully activated under most conditions (e.g. Fig. 2E), consistent with previous studies (20, 23, 31), the Boltzmann fits obtained here may have been biased towards the hyperpolarized direction. Furthermore, because the g_{max} values reported here were the results of extrapolation, they should be interpreted with caution. We have presented statistical analyses for current density at 110 mV in parallel with g_{max}, and prefer to put more weight on the current density than g_{max} when interpreting our results.

Together, our results establish for the first time the role of SMS1 in the regulation of KCNQ1/KCNE1 channels. These results are of broad biological significance because of the important roles played by KCNQ1/KCNE1 channels in a number of organs, including the inner ear (14, 21), heart (5, 30, 42), pancreas (13, 45), and brain (10).

Mechanism underlying the regulation of KCNQ1/KCNE1 channels by SMS1

SMS catalyzes the conversion of phosphatidylcholine and ceramide to sphingomyelin and DAG. Two isoforms of SMS (SMS1 and SMS2) have been identified; SMS2 is found in the cytoplasmic membrane, whereas SMS1 is primarily localized in the Golgi apparatus (18, 38). Both isoforms are shown here to be expressed in HEK293T cells, but the focus here is on SMS1. Manipulation of SMS1 activity is expected to change the level of all four molecules in the reaction it catalyzes, as well as other phospholipids in related networks (11, 20). The question is, therefore, which of these molecules mediates the effect of SMS1 manipulation on KCNQ1/KCNE1?

Sphingomyelin may appear as the immediate candidate. Indeed, a growing body of evidence suggests that membrane lipids regulate voltage-dependent ion channels. Sphingomyelin, in particular its phospho-head group, is essential for the proper gating of certain voltage-dependent K^+ channels (28, 44). Another phospholipid, phosphatidylinositol 4,5-bisphosphate (PIP_2), is critical for KCNQ channel opening (reviewed in Ref. 47). Furthermore, recent studies investigating the mechanism underlying the effect of lipids on channels have revealed that polyunsaturated fatty acid analogs modulate cardiac I_{Ks} channel functions via an electrostatic mechanism (20); the negative or positive charges of the fatty acids change channel voltage dependence by acting electrostatically on the channel voltage sensor (7). In all these studies, a common effect of lipids is to affect channel gating. In the present study, however, in response to manipulation of SMS1

353 expression, we observed only changes in channel density, but not in voltage
354 dependence or channel kinetics. The mechanism for the regulation of
355 KCNQ1/KCNE1 channels by SMS1 must be one that controls membrane protein
356 level.

357 Here, we focused on DAG, because binding of DAG is known to recruit PKD
358 to the trans-Golgi network, thereby promoting protein transport to the cell
359 membrane (6, 22). Although the modulation of SMS1 activity does not change the
360 total cellular level of DAG (39, 41), DAG expression in the Golgi is reduced in
361 SMS-knockdown cells and increased in SMS-overexpressing cells (41). Villani et al.
362 (2008) also demonstrated a reduction in localization of the DAG-binding kinase PKD
363 to the Golgi. Further, in HeLa cells, the vesicular stomatitis virus G protein was used
364 as a reporter protein to reveal that SMS regulates trans-Golgi network-mediated
365 protein trafficking (37). In line with this evidence, our results show that PKD
366 inhibition suppresses KCNQ1/KCNE1 channel density, but not after knockdown of
367 SMS1.

368 However, the DAG analogue PMA appeared to have no effect on current
369 density. DAG activates not only PKD but also PKC (reviewed in Ref. 46), and there is
370 evidence that PKC activity is required for PKD activation (8, 49). Because PKC has
371 also been reported to affect KCNQ1/KCNE1 channels (17, 43), PMA appears not to
372 simply mimic the effect of SMS1 on KCNQ1/KCNE1, but may affect the channels
373 through multiple mechanisms. In fact, previous studies on the action of phorbol
374 esters on KCNQ1/KCNE1 channels in cells other than HEK293T have reported either

enhancement (43) or suppression (17). Compared with DAG, the effect of PKD can be addressed more specifically using selective inhibitors. The PKD inhibitors used here have been shown to inhibit PKD selectively, with little effect on PKC (9, 33).

To conclude, the present results suggest that SMS1 positively regulates KCNQ1/KCNE1 channel expression without changing channel properties. Our data provide evidence in support of a working hypothesis that SMS1 upregulates KCNQ1/KCNE1 channel density via DAG-binding PKD.

Acknowledgment

This work was supported by grants from the Japan Society for the Promotion of Science (#25290006, #25670719, and #15H01442).

References

1. **Abbott GW.** Biology of the KCNQ1 potassium channel. *New J Sci* 2014: article ID: 237431, 2014.
2. **Adibhatla RM, Hatcher JF, Gusain A.** Tricyclodecan-9-yl-xanthogenate (D609) mechanism of actions: a mini-review of literature. *Neurochem Res* 37: 671-679, 2012.
3. **Anantharam A, Markowitz SM, Abbott GW.** Pharmacogenetic considerations in diseases of cardiac ion channels. *J Pharmacol Exp Ther* 307: 831–838, 2003.

4. **Barceló-Coblijn G, Martin ML, de Almeida RF, Noguera-Salvà MA, Marcilla-Etxenike A, Guardiola-Serrano F, Lüth A, Kleuser B, Halver JE, Escribá PV**. Sphingomyelin and sphingomyelin synthase (SMS) in the malignant transformation of glioma cells and in 2-hydroxyoleic acid therapy. *Proc Natl Acad Sci U S A* 108:19569-19574, 2011.

5. **Barhanin J, Lesage F, Guillemare E, Fink M, Lazdunski M, Romey G.** KVLQT1 and IsK (minK) proteins associate to form the IKs cardiac potassium current. *Nature* 384, 78–80, 1996.

6. **Baron CL, Malhotra V.** Role of diacylglycerol in PKD recruitment to the TGN and protein transport to the plasma membrane. *Science* 295: 325-328, 2002.

7. **Börjesson SI, Parkkari T, Hammarström S, Elinder F.** Electrostatic tuning of cellular excitability. *Biophys J* 98: 396–403, 2010.

8. **Díaz Añel AM, Malhotra V**. PKCeta is required for beta1gamma2/beta3gamma2- and PKD-mediated transport to the cell surface and the organization of the Golgi apparatus. *J Cell Biol* 169:83-91, 2005.

9. **George KM, Frantz MC, Bravo-Altamirano K, Lavalle CR, Tandon M, Leimgruber S, Sharlow ER, Lazo JS, Wang QJ, Wipf P**. Design, synthesis, and biological evaluation of PKD inhibitors. *Pharmaceutics* 3:186-228, 2011.

10. **Goldman AM1, Glasscock E, Yoo J, Chen TT, Klassen TL, Noebels J.** Arrhythmia in heart and brain: KCNQ1 mutations link epilepsy and sudden unexplained death. *Sci Transl Med* 1: 2-6, 2009.

11. **Hannun YA, Obeid LM.** The Ceramide-centric universe of lipid-mediated cell

regulation: stress encounters of the lipid kind. *JBiol Chem* 277: 25847-25850, 2002.

12. **Hattori S, Murakami F, and Song W-J.** Quantitative relationship between between Kv4.2 mRNA and A-type potassium current in rat striatal cholinergic interneurons during postnatal development. *JNeurophysiol* 90: 175-183, 2003.
13. **Hayashi M, Novak I.** Molecular basis of potassium channels in pancreatic duct epithelial cells. *Channels* 7: 432–441, 2013.
14. **Hibino H, Nin F, Tsuzuki C, Kurachi Y.** How is the highly positive endocochlear potential formed? The specific architecture of the stria vascularis and the roles of the ion-transport apparatus. *Pflugers Arch* 459: 521–533, 2010.
15. **Jespersen T, Grunnet M, Olesen SP.** The KCNQ1 potassium channel: from gene to physiological function. *Physiology (Bethesda)* 20: 408–416, 2005.
16. **Jin ZX, Huang CR, Dong L, Goda S, Kawanami T, Sawaki T, Sakai T, Tong XP, Masaki Y, Fukushima T, Tanaka M, Mimori T, Tojo H, Bloom ET, Okazaki T, Umehara H.** Impaired TCR signaling through dysfunction of lipid rafts in sphingomyelin synthase 1 (SMS1)-knockdown T cells. *Int Immunol* 20: 1427-1437, 2008.
17. **Kanda VA, Purtell K, Abbott GW**. Protein kinase C downregulates I(Ks) by stimulating KCNQ1-KCNE1 potassium channel endocytosis. *Heart Rhythm* 8:1641-1647, 2011.
18. **Kitatani K, Taniguchi M, Okazaki T.** Role of sphingolipids and metabolizing enzymes in hematological malignancies. *Mol Cells* 38: 482-495, 2015.
19. **Liin SI, Barro-Soria R, Larsson HP.** The KCNQ1 channel - remarkable flexibility

441 in gating allows for functional versatility. *J Physiol* 593: 2605-15, 2015.

442 20. **Liin SI, Silverå Ejneby M, Barro-Soria R, Skarsfeldt MA, Larsson JE, Starck**
443 **Härlin F, Parkkari T, Bentzen BH, Schmitt N, Larsson HP, Elinder F.**
444 Polyunsaturated fatty acid analogs act antiarrhythmically on the cardiac IKs
445 channel. *Proc Natl Acad Sci U S A* 112: 5714-5719, 2015.

446 21. **Lu M-H, Takemoto M, Watanabe K, Luo H, Nishimura M, Yano M, Tomimoto**
447 **H, Okazaki T, Oike Y, Song W-J.** Deficiency of sphingomyelin synthase-1 but not
448 sphingomyelin synthase-2 causes hearing impairments in mice. *J Physiol* 590:
449 4029-4044, 2012.

450 22. **Malhotra V, Campelo F.** PKD regulates membrane fission to generate TGN to cell
451 surface transport carriers. *Cold Spring Harb Perspect Biol* 3(2). pii: a005280, 2011.

452 23. **Moreno C, de la Cruz A, Oliveras A, Kharche SR, Guizy M, Comes N, Starý T,**
453 **Ronchi C, Rocchetti M, Baró I, Loussouarn G, Zaza A, Severi S, Felipe A,**
454 **Valenzuela C**. Marine n-3 PUFAs modulate IKs gating, channel expression, and
455 location in membrane microdomains. *Cardiovasc Res*. 105:223-232, 2015.

456 24. **Murai T, Kakizuka A, Takumi T, Ohkubo H, Nakanishi S.** Molecular cloning
457 and sequence analysis of human genomic DNA encoding a novel membrane
458 protein which exhibits a slowly activating potassium channel activity. *Biochem*
459 *Biophys Res Commun* 161: 176-181, 1989.

460 25. **Nakajo K, Kubo Y.** KCNQ1 channel modulation by KCNE proteins via the
461 voltage-sensing domain. *J Physiol* 593: 2617-2625, 2015.

462 26. **Nerbonne JM, Kass RS.** Molecular physiology of cardiac repolarization. *Physiol*

Rev 85: 1205–1253, 2005.

27. **Neyroud N, Tesson F, Denjoy I, LeiboviciM,Donger C, Barhanin J, Faure S, Gary F, Coumel P, Petit C, Schwartz K, Guicheney P.** A novel mutation in the potassium channel gene KVLQT1 causes the Jervell and Lange-Nielsen cardioauditory syndrome. *Nat Gen* 15: 186–189, 1997.

28. **Ramu Y, Xu Y, Lu Z.** Enzymatic activation of voltage-gated potassium channels. *Nature* 442: 696–699, 2006.

29. **Sakagami M, Fukazawa K, Matsunaga T, Fujita H, Mori N, Takumi T, Ohkubo H, Nakanishi S.** Cellular localization of rat Isk protein in the stria vascularis by immunohistochemical observation. *Hear Res* 56: 168-172, 1991.

30. **Sanguinetti MC, Curran ME, Zou A, Shen J, Spector PS, Atkinson DL, Keating MT.** Coassembly of KVLQT1 and minK (IsK) proteins to form cardiac IKs potassium channel. *Nature* 384: 80–83, 1996.

31. **Seebohm G, Strutz-Seebohm N, Birkin R, Dell G, Bucci C, Spinosa MR, Baltaev R, Mack AF, Korniychuk G, Choudhury A, Marks D, Pagano RE, Attali B, Pfeufer A, Kass RS, Sanguinetti MC, Tavare JM, Lang F**. Regulation of endocytic recycling of KCNQ1/KCNE1 potassium channels. *Circ Res*. 100: 686-692, 2007.

32. **Schroeder BC,Waldegger S, Fehr S, Bleich M,Warth R, Greger R, Jentsch TJ.** A constitutively open potassium channel formed by KCNQ1 and KCNE3. *Nature* 403: 196–199, 2000.

33. **Sharlow ER, Giridhar KV, LaValle CR, Chen J, Leimgruber S, Barrett R,**

Bravo-Altamirano K, Wipf P, Lazo JS, Wang QJ. Potent and selective disruption of protein kinase D functionality by a benzoxoloazepinolone. *J Biol Chem* 283:33516-33526, 2008.

34. **Sharlow ER1, Mustata Wilson G, Close D, Leimgruber S, Tandon M, Reed RB, Shun TY, Wang QJ, Wipf P, Lazo JS**. Discovery of diverse small molecule chemotypes with cell-based PKD1 inhibitory activity. *PLoS One* 6(10):e25134, 2011.

35. **Song W-J, Baba Y, Otsuka T, Murakami F.** Characterization of Ca^{2+} channels in rat subthalamic nucleus neurons. *J Neurophysiol* 84: 2630-2637, 2000.

36. **Song W-J, Tkatch T, Baranauskas G, Ichinohe N, Kitai S, Surmeier DJ.** Somatodendritic depolarization-activated potassium currents in rat neostriatal cholinergic interneurons are predominantly of the A-type and attributable to co-expression of Kv4.2 and Kv4.1 subunits. *J Neurosci* 18: 3124-3137, 1998.

37. **Subathra M, Qureshi A, Luberto C.** Sphingomyelin synthases regulate protein trafficking and secretion. *PLoS One* 6: e23644, 2011.

38. **Tafesse FG, Ternes P, Holthuis JC.** The multigenic sphingomyelin synthase family. *J Biol Chem* 281: 29421–29425, 2006.

39. **Tafesse F, Huitema K, Hermansson M, van der Poel S, van den Dikkenberg J, Uphoff A, Somerharju P, Holthuis J.** Both sphingomyelin synthases SMS1 and SMS2 are required for sphingomyelin homeostasis and growth in human HeLa cells. *J Biol Chem* 282: 17537–17547, 2007.

40. **Takumi T, Ohkubo H, Nakanishi S.** Cloning of a membrane protein that induces

507 a slow voltage-gated potassium current. *Science* 242: 1042-1045, 1988.

508 41. **Villani M, Subathra M, Im YB, Choi Y, Signorelli P, Del Poeta M, Luberto C.**

509 Sphingomyelin synthases regulate production of diacylglycerol at the Golgi.

510 *Biochem J* 414: 31-41, 2008.

511 42. **Wang KW, Tai KK, Goldstein SA.** MinK residues line a potassium channel pore.

512 *Neuron* 16: 571–577, 1996.

513 43. **Xiao GQ, Mochly-Rosen D, Boutjdir M**. PKC isozyme selective regulation of

514 cloned human cardiac delayed slow rectifier K current. *Biochem Biophys Res*

515 *Commun* 306:1019-1025, 2003.

516 44. **Xu Y, Ramu Y, Lu Z.** Removal of phospho-head groups of membrane lipids

517 immobilizes voltage sensors of K^+ channels. *Nature* 451: 826–830, 2008.

518 45. **Yamagata K, Senoguchi T, Lu M-H, Takemoto M, Karim F, Go C, Sato Y, Hatta**

519 **M, Yoshizawa T, Araki E, Miyazaki J, Song W-J.** Voltage-gated K^+ channel

520 KCNQ1 regulates insulin secretion in MIN6 beta-cell line. *Biochem Biophys Res*

521 *Comm* 407: 620-625, 2011.

522 46. **Yang C, Kazanietz MG.** Divergence and complexities in DAG signaling: looking

523 beyond PKC. *Trends Pharmacol Sci* 24:602-608, 2003.

524 47. **Zaydman MA, Cui J.** PIP2 regulation of KCNQ channels: biophysical and

525 molecular mechanisms for lipid modulation of voltage-dependent gating. *Front*

526 *Physiol* 5: 195, 2014.

527 48. **Zhao S, Zhou L, Niu G, Li Y, Zhao D, Zeng H**. Differential regulation of orphan

528 nuclear receptor TR3 transcript variants by novel vascular growth factor

signaling pathways. *FASEB J* 28:4524-4533, 2014.

49. **Zugaza J L, Sinnett-Smith J, Van Lint J, Rozengurt E.** Protein kinase D (PKD) activation in intact cells through a protein kinase C-dependent signal transduction pathway. *EMBO J* 15: 6220–6230, 1996.

Figure Legends

Fig. 1. Expression of KCNQ1/KCNE1 channels in HEK293T cells. (A) K^+ currents evoked in a HEK293T cell, with voltage steps from −60 mV to +50 mV at a 10-mV interval (inset: protocol). (B) K^+ currents evoked with the protocol shown in (A, inset), in a cell transfected with KCNQ1 alone. (C) K^+ currents in a cell transfected with KCNQ1 and KCNE1. Arrow points to tail currents at −40 mV. (D) Current density in the three cell groups at different voltages. **$p < 0.01$ vs. no transfection and vs. KCNQ1 transfection. Cell capacitances for the control, KCNQ1, and KCNQ1/KCNE1 groups were 17.9 ± 1.6 pF, 14.0 ± 1.2 pF, and 13.6 ± 1.3 pF, respectively; no statistical difference in cell capacitance was found between groups in this or any other figure.

Fig. 2. Effect of D609 on KCNQ1/KCNE1 currents. Currents shown here and in all subsequent figures were evoked with the voltage protocol shown in Fig. 1A (inset), except that the highest voltage was increased to 110 mV. (A) Currents from a cell cultured in control conditions. (B) Currents from a cell that had received D609 before recording. (C) Current densities of the control and D609-treated groups; ***$p < 0.001$.

Cell capacitances were 16.2 ± 1.6 pF and 12.0 ± 2.3 pF for the control and D609 groups, respectively. (D) Conductance density–voltage relationship in a control cell and a D609-treated cell. Boltzmann fit parameters are shown for each cell. (E) Boltzmann fits for the two cells in (D) are shown with normalized maximum conductance density. D609 induced a marked shift in voltage dependence. (F) Box plots for maximum conductance density (g_{max}), half activation voltage (V_h), and slope factor (V_c); open circles represent outliers. n = 10 (control) or 9 (D609); **p < 0.01.

Fig. 3. SMS1 downregulation reduced KCNQ1/KCNE1 current density. (A) Effect of SMS1 knockdown on mRNA levels of SMS1 and SMS2. Fluorescence ratios of SMS1 and SMS2 to beta-actin cDNA in the control and shRNA groups were normalized to the control for SMS1. Inset, photograph showing SMS1 RT-PCR products in a control sample (SMS1-ctrl) and a SMS1 knockdown sample (SMS1-KD), together with products of beta-actin; *p < 0.05, n = 7 for SMS1 and SMS2. (B) Currents from a control cell. (C) Currents from an SMS1 knockdown cell. (D) Voltage-dependent current density in the control and knockdown groups; *p < 0.05. Cell capacitances were 13.7 ± 1.3 pF and 13.5 ± 1.3 pF for the control and shRNA groups, respectively.

Fig. 4. SMS1 downregulation did not change channel voltage dependence or channel kinetics. (A) Conductance density–voltage relationship of a control cell transfected with scrambled RNA and a knockdown cell transfected with SMS1 shRNA. Boltzmann fit parameters are shown for each cell. (B) Box plots for maximum

573 conductance density (g_{max}), half activation voltage (V_h), and slope factor (V_c); open
574 circles represent outliers. n = 24 (control) or 24 (knockdown); *p < 0.05. (C) Currents
575 evoked by a voltage step to 110 mV in 15 control cells, normalized to the maximum
576 value. Heavy line, mean; fine lines, mean ± 2SD. (D) Difference current between the
577 means of the control and knockdown groups (n = 15). Heavy line, difference in mean
578 currents; fine lines, ± 2SD for the control condition; the difference current during and
579 after the voltage step never exceeded the 2SD range, suggesting a lack of statistical
580 difference between control and knockdown conditions.
581
582 Fig. 5. SMS1 overexpression increased KCNQ1/KCNE1 current density. (A) Effect of
583 SMS1 overexpression on SMS1 and SMS2 mRNA levels. Fluorescence ratios of SMS1
584 and SMS2 to beta-actin cDNA in the control and overexpression groups, normalized
585 to the control for SMS1. Inset, photograph showing SMS1 and beta-actin RT-PCR
586 products in a control sample and an overexpression sample. *p < 0.05, n = 6 (SMS1
587 and SMS2). (B) Currents from a control cell transfected with the empty vector. (C)
588 Currents from a cell transfected with SMS1. (D) Voltage-dependent current density
589 of control and overexpression groups. *p < 0.05. Cell capacitances were 13.9 ± 5.2 pF
590 and 12.0 ± 0.7 pF for the control and overexpression groups, respectively.
591
592 Fig. 6. PKD inhibition reduced KCNQ1/KCNE1 current density. (A) Control cell
593 currents. (B) Currents from a cell treated with the PKD inhibitor CID-755673 for 6 h
594 before recording. (C) Current density in the control and CID-755673-treated groups;

595 *p < 0.05. Cell capacitances were 16.0 ± 1.7 pF and 17.8 ± 1.5 pF for the control and
596 CID-755673 groups, respectively. (D) Conductance density–voltage relationship in a
597 control cell and a CID-755673-treated cell. Boltzmann fit parameters are shown for
598 each cell. (E) Box plots of maximum conductance density (g_{max}), half activation
599 voltage (V_h), and slope factor (V_c); open circles represent outliers. n = 14 (control) or
600 12 (CID-755673); *p < 0.05.
601
602 Fig. 7. Non-additive effects of SMS1 knockdown and PKD inhibition. (A) Currents in
603 a control cell transfected with scrambled RNA. (B) Currents in a cell transfected with
604 SMS1 shRNA. (C) Currents in a cell transfected with SMS1 shRNA and treated with
605 CID-755673. (D) Current density–voltage relationships in the three groups; *p < 0.05
606 for control vs. SMS1 shRNA and for control vs. (SMS1 shRNA + CID-755673). Cell
607 capacitances were 16.0 ± 1.7 pF, 15.4 ± 1.2 pF, and 18.4 ± 1.9 pF for the control, shRNA,
608 and shRNA+CID-755673 groups, respectively.
609
610
611

Fig. 1

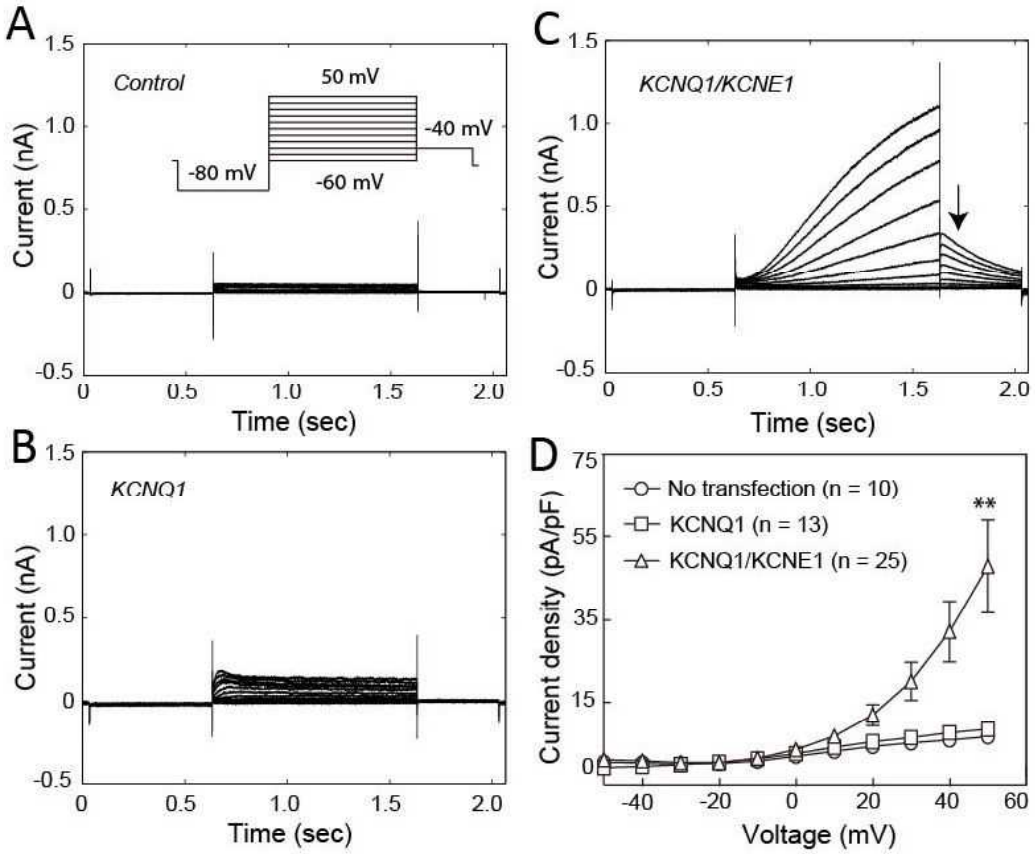
A
Control
50 mV
-40 mV
-80 mV
-60 mV
Current (nA)
Time (sec)
B
KCNQ1
Current (nA)
Time (sec)
C
KCNQ1/KCNE1
Current (nA)
Time (sec)
D
No transfection (n = 10)
KCNQ1 (n = 13)
KCNQ1/KCNE1 (n = 25)
**
Current density (pA/pF)
Voltage (mV)

Fig. 2

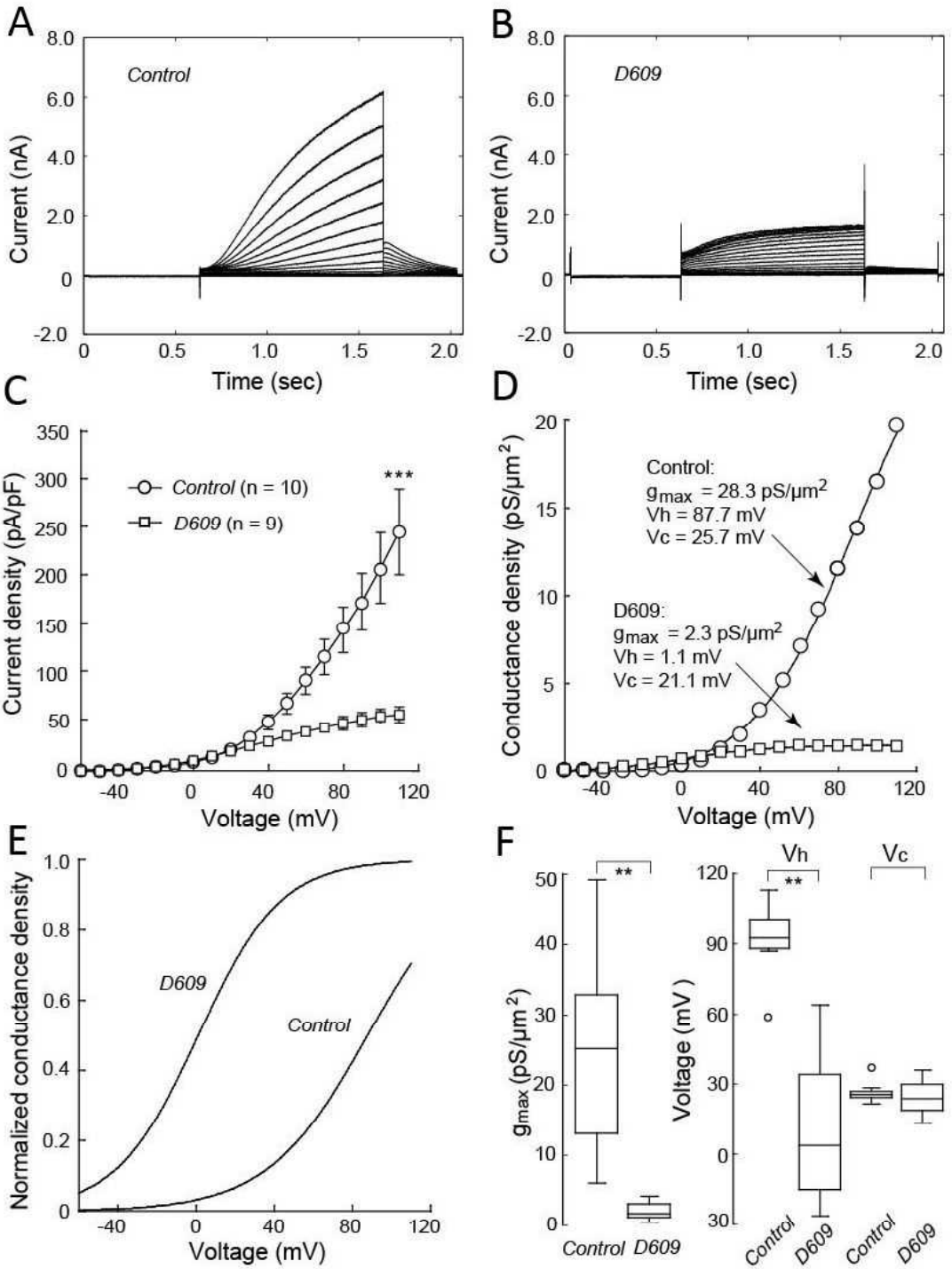
A
Control
Current (nA)
Time (sec)
B
D609
Current (nA)
Time (sec)
C
Control (n = 10)
D609 (n = 9)
***
Current density (pA/pF)
Voltage (mV)
D
Control:
gmax = 28.3 pS/μm2
Vh = 87.7 mV
Vc = 25.7 mV
D609:
gmax = 2.3 pS/μm2
Vh = 1.1 mV
Vc = 21.1 mV
Conductance density (pS/μm2)
Voltage (mV)
E
D609
Control
Normalized conductance density
Voltage (mV)
F
Vh
Vc
**
**
gmax (pS/μm2)
Voltage (mV)
Control
D609
Control
D609
Control
D609

Fig. 3

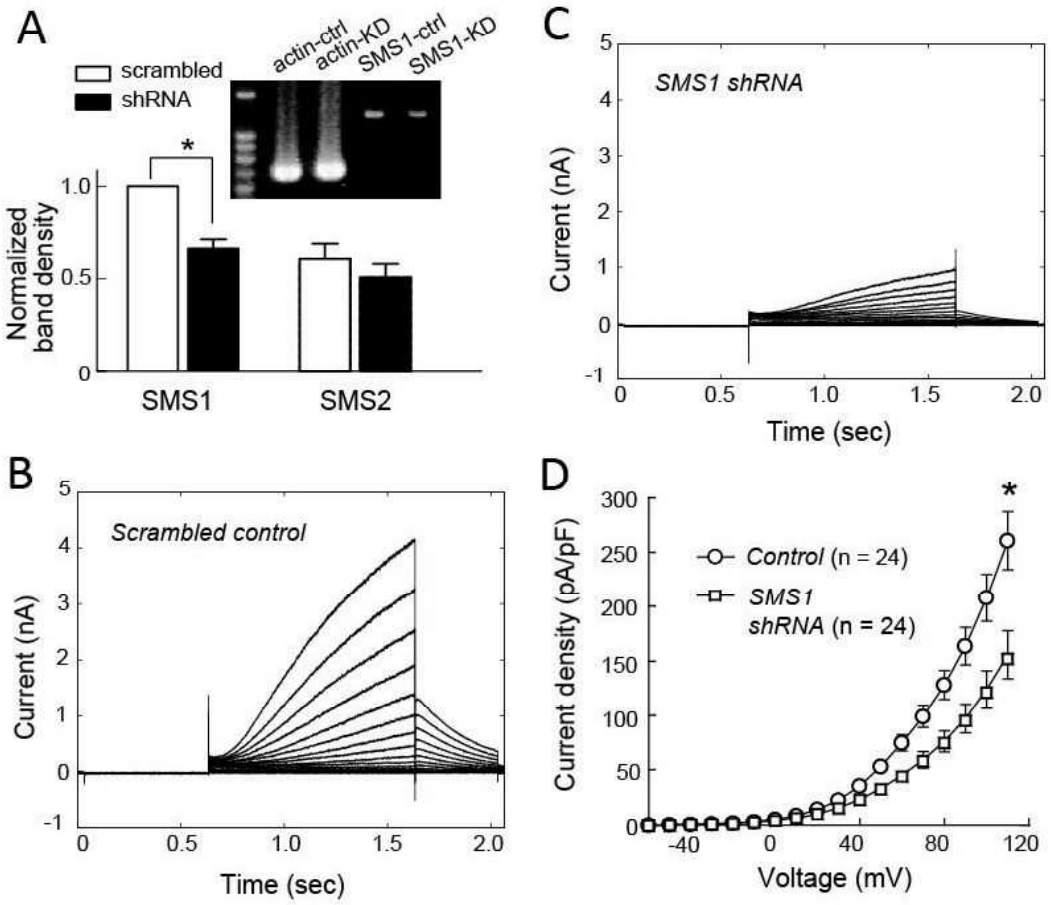
A
scrambled
shRNA
actin-ctrl
actin-KD
SMS1-ctrl
SMS1-KD
*
Normalized band density
1.0
0.5
0
SMS1
SMS2
B
Scrambled control
Current (nA)
Time (sec)
C
SMS1 shRNA
Current (nA)
Time (sec)
D
*
Control (n = 24)
SMS1 shRNA (n = 24)
Current density (pA/pF)
Voltage (mV)

Fig. 4

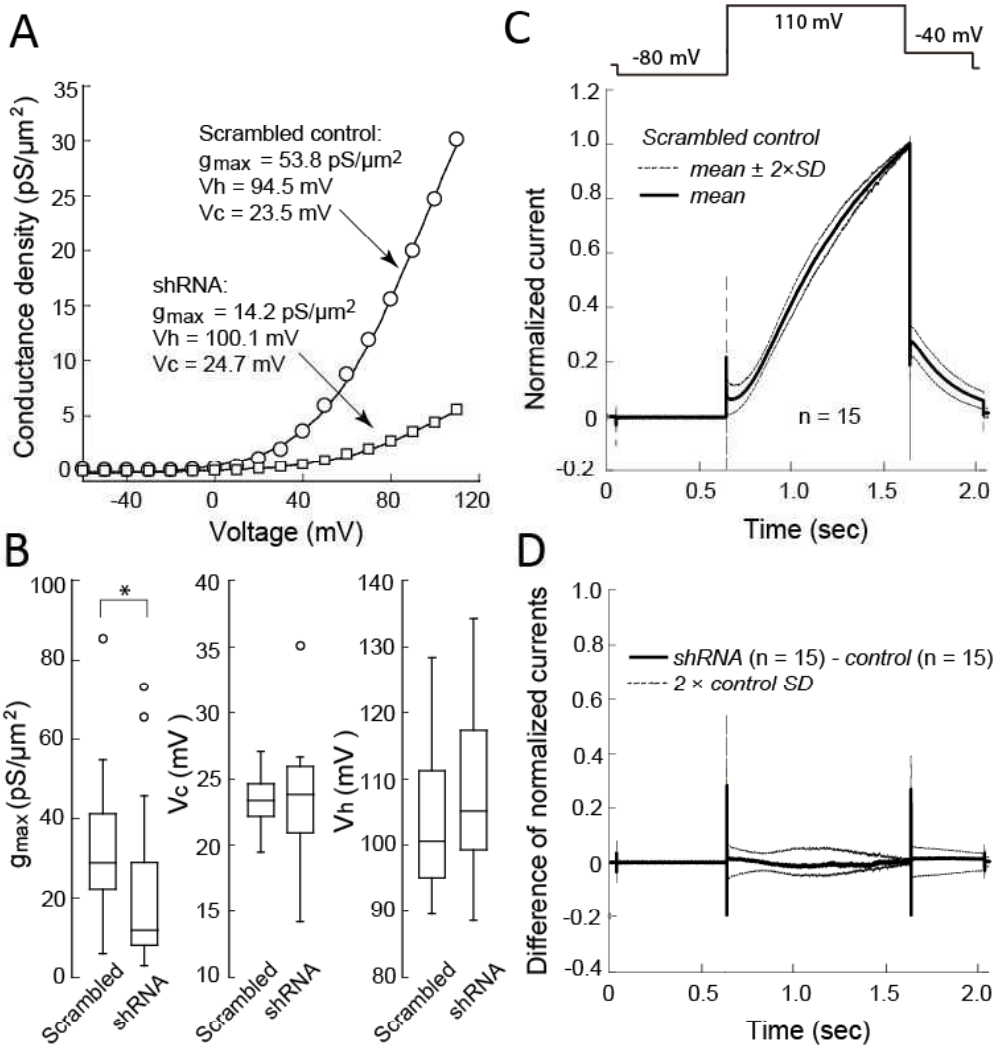
A
Conductance density (pS/μm²)
Scrambled control:
gmax = 53.8 pS/μm²
Vh = 94.5 mV
Vc = 23.5 mV
shRNA:
gmax = 14.2 pS/μm²
Vh = 100.1 mV
Vc = 24.7 mV
Voltage (mV)
B
gmax (pS/μm²)
Vc (mV)
Vh (mV)
Scrambled
shRNA
C
-80 mV
110 mV
-40 mV
Scrambled control
mean ± 2×SD
mean
Normalized current
n = 15
Time (sec)
D
shRNA (n = 15) - control (n = 15)
2 × control SD
Difference of normalized currents
Time (sec)

Fig. 5

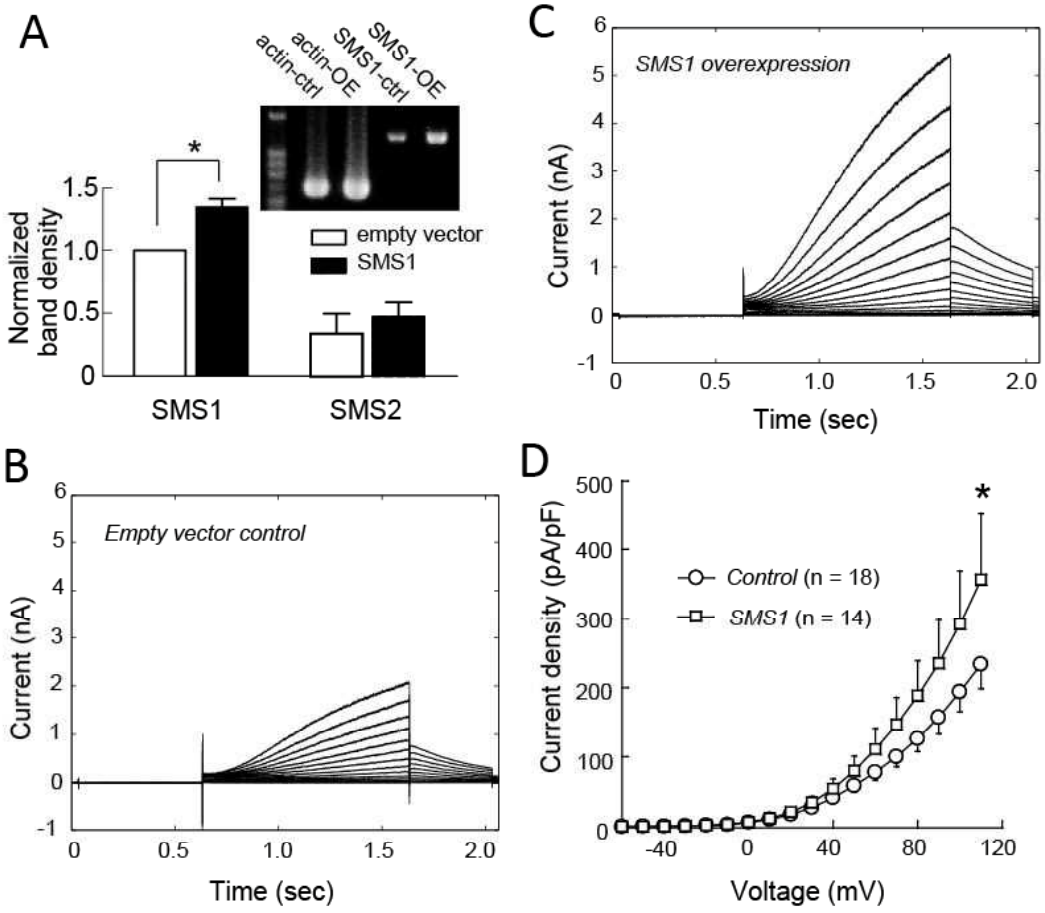
A
actin-ctrl
actin-OE
SMS1-ctrl
SMS1-OE
*
Normalized band density
1.5
1.0
0.5
0
empty vector
SMS1
SMS1
SMS2
B
Empty vector control
Current (nA)
Time (sec)
C
SMS1 overexpression
Current (nA)
Time (sec)
D
Current density (pA/pF)
Control (n = 18)
SMS1 (n = 14)
*
Voltage (mV)

Fig. 6

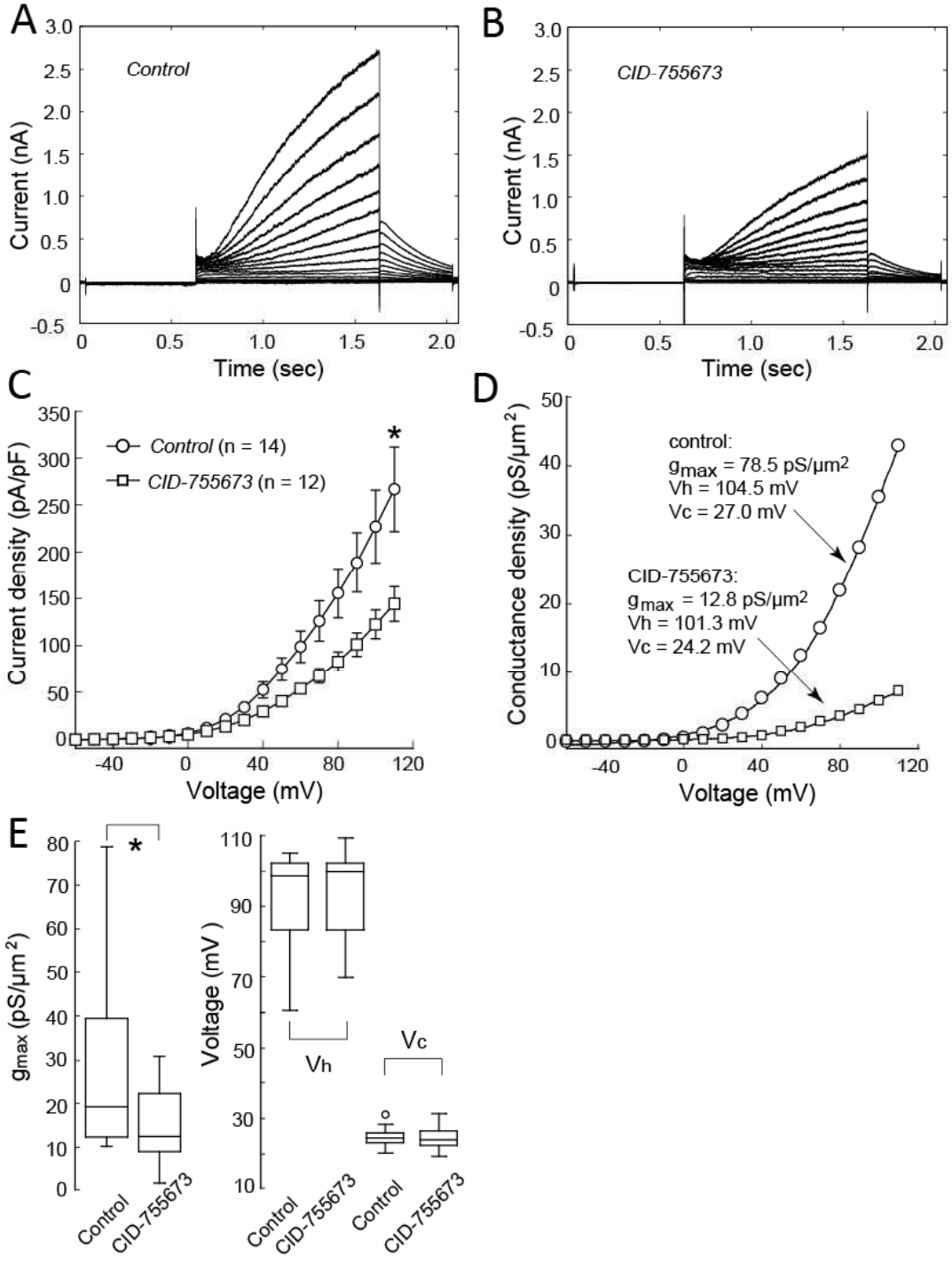
A
Control
Current (nA)
Time (sec)
B
CID-755673
Current (nA)
Time (sec)
C
Control (n = 14)
CID-755673 (n = 12)
*
Current density (pA/pF)
Voltage (mV)
D
control:
gmax = 78.5 pS/μm2
Vh = 104.5 mV
Vc = 27.0 mV
CID-755673:
gmax = 12.8 pS/μm2
Vh = 101.3 mV
Vc = 24.2 mV
Conductance density (pS/μm2)
Voltage (mV)
E
*
gmax (pS/μm2)
Control
CID-755673
Voltage (mV)
Vh
Vc
Control
CID-755673
Control
CID-755673

Fig. 7

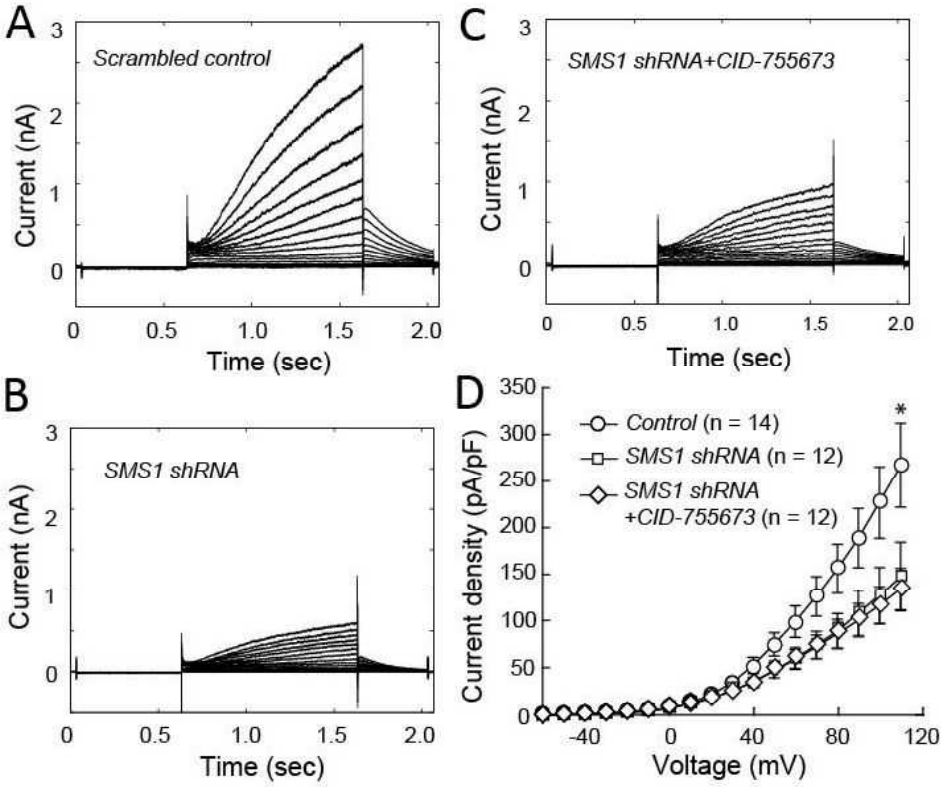
A
Scrambled control
Current (nA)
Time (sec)
B
SMS1 shRNA
Current (nA)
Time (sec)
C
SMS1 shRNA+CID-755673
Current (nA)
Time (sec)
D
Control (n = 14)
SMS1 shRNA (n = 12)
SMS1 shRNA
+CID-755673 (n = 12)
*
Current density (pA/pF)
Voltage (mV)